RADIATION RESEARCH **154**, 547–555 (2000)
0033-7587/00 $5.00

Optical Sensor-Based Oxygen Tension Measurements Correspond with Hypoxia Marker Binding in Three Human Tumor Xenograft Lines

J. Bussink,[a,1] J. H. A. M. Kaanders,[a] A. M. Strik,[a] B. Vojnovic[b] and A. J. van der Kogel[a]

[a] *Department of Radiation Oncology, UMC St Radboud, Joint Centre for Radiation Oncology Arnhem-Nijmegen, P.O. Box 9101, 6500 HB Nijmegen, The Netherlands; and* [b] *Gray Laboratory Cancer Research Trust, P.O. Box 100, Mount Vernon Hospital, Northwood, Middlesex, HA6 2JR, United Kingdom*

Bussink, J., Kaanders, J. H. A. M., Strik, A. M., Vojnovic, B. and van der Kogel, A. J. Optical Sensor-Based Oxygen Tension Measurements Correspond with Hypoxia Marker Binding in Three Human Tumor Xenograft Lines. ***Radiat. Res.*** **154, 547–555 (2000).**

Hypoxia has a negative effect on the outcome of radiotherapy and surgery and is also related to an increased incidence of distant metastasis. In this study, tumor pO_2 measurements using a newly developed time-resolved luminescence-based optical sensor (OxyLite™) were compared with bioreductive hypoxia marker binding (pimonidazole). Single pO_2 measurements per tumor were compared to hypoxia marker binding in tissue sections using image analysis. Both assays were performed in the same tumors of three human tumor lines grown as xenografts. Both assays demonstrated statistically significant differences in the oxygenation status of the three tumor lines. There was also a good correlation between hypoxia marker binding and the pO_2 measurements with the OxyLite™ device. A limitation of the OxyLite™ system is that it is not yet suited for sampling multiple sites in one tumor. An important strength is that continuous measurements can be taken at the same position and dynamic information on the oxygenation status of tumors can be obtained. The high spatial resolution of the hypoxia marker binding method can complement the limitations of the OxyLite™ system. In the future, a bioreductive hypoxic cell marker for global assessment of tumor hypoxia may be combined with analysis of temporal changes in pO_2 with the OxyLite™ to study the effects of oxygenation-modifying treatment on an individual basis.

INTRODUCTION

It is well known that radiotherapy under hypoxic conditions is less effective than under conditions of normal oxygenation (*1, 2*). Hypoxia is currently considered to be one of the three most important mechanisms of radiation resistance together with intrinsic radioresistance and rapid cell proliferation. The importance of tumor hypoxia for the outcome of radiation treatment has been illustrated by treatment strategies with the aim of overcoming tumor hypoxia. The use of hyperbaric oxygen, carbogen breathing, vasoactive drugs and hypoxic cell sensitizers in combination with radiotherapy have shown an increase in local-regional control and sometimes survival (*3–7*). The oxygenation status of tumors is an important indicator not only for the outcome of radiotherapy, but also for surgical treatment, as has been shown for cancer of the uterine cervix (*8*). Finally, hypoxia has been correlated with an increased incidence of distant metastases in human soft tissue sarcomas (*9*) and carcinoma of the uterine cervix (*10*). The negative effect of hypoxia on the outcome of radiation treatment can be explained by the lower amount of radical damage in a hypoxic environment. The adverse correlation with the outcome of surgical treatment and the increased incidence of metastases in hypoxic tumors could be the result of the expression of certain oncogenes or stress proteins or production of cytokines stimulated by low oxygen tensions (*11*). It has been shown that hypoxia can elevate the mutation frequency in cultured cells, thereby acting as a mechanism for tumor progression (*12*).

Tumor hypoxia can be analyzed in various ways. Radiobiological hypoxia can be assessed with the paired survival curve assay (*13, 14*) and with the comet assay (*15*). Direct measurement of tumor tissue oxygenation is possible with polarographic needle electrodes (Eppendorf™) (*16–18*) or time-resolved luminescence-based optical sensors (*19, 20*). Other methods to study hypoxia in tissues include the use of bioreductive chemical probes such as the 2-nitroimidazoles (*21–23*), electron paramagnetic resonance oximetry (*24*), and cryospectrophotometry of intravascular HbO_2 saturation (*25*).

A number of studies have shown a correlation between hypoxia assessed by polarographic measurements (Eppendorf™) and the outcome of radiotherapy (*17, 18, 26, 27*).

[1] Author to whom correspondence should be addressed at Department of Radiation Oncology, UMC St Radboud, Geert Grooteplein 32, P.O. Box 9101, 6500 HB Nijmegen, The Netherlands.

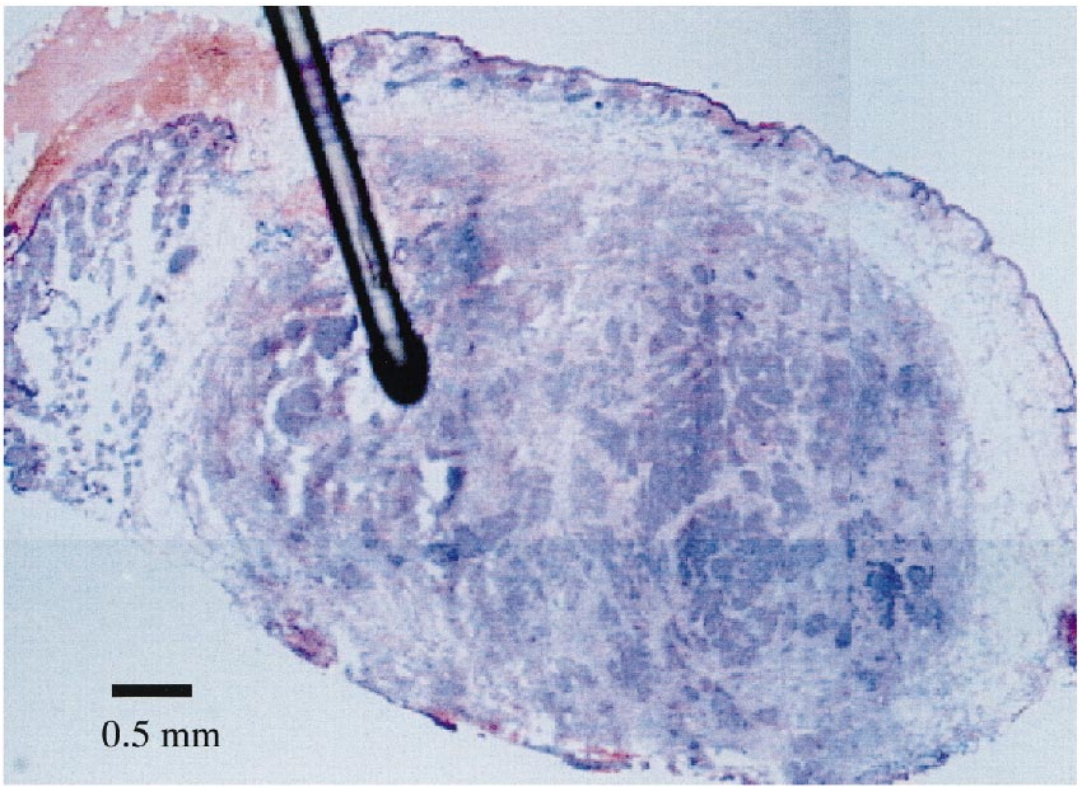

FIG. 1. Example of an H&E-stained section of the human squamous cell carcinoma xenograft tumor line SCCNij3 with a fiber-optic oxygen probe overlaid. The photomicrograph shows the dimensions of the probe relative to tissue architecture.

However, a disadvantage of this method is that temporal changes in oxygenation cannot be measured reliably because the microelectrode cannot be left in the same position within the tumor for prolonged periods. The reason for this is that during the polarographic pO_2 measurements small amounts of oxygen are consumed and a diffusion gradient is generated. The electrode therefore needs to be moved through the tissue to prevent development of hypoxia as an artifact of the measurements (*28, 29*).

Recently a fiber-optic probe was developed for pO_2 measurements. The pO_2 measurements with this method are based on pO_2-dependent changes in the half-life of an excited luminophore at the tip of a probe. This process does not consume oxygen but relies only on the presence of oxygen[2] (*19, 20*). The fiber-optic probe can be left at one position for a longer period, which makes it possible to measure the effect of oxygenation-modifying interventions over time in a tissue.

In the present study, we compared tumor pO_2 measurements using time-resolved luminescence-based optical sensors (OxyLite™) with bioreductive hypoxia marker binding (pimonidazole) in tissue sections using a semi-automatic computer-controlled method for simultaneous multiparameter analysis of whole tissue sections (*30–32*). Both assays were performed in the same tumors of three different human tumor lines grown as xenografts in nude mice.

[2] W. K. Young, B. Vojnovic, J. Bussink, A. J. van der Kogel, R. J. Locke and P. Wardman, manuscript submitted for publication.

MATERIALS AND METHODS

Tumors

Three human xenograft tumor lines (SCCNij3, E102 and E106) with different vascular architecture and widely different distribution patterns of hypoxia were used for these experiments. Tumor line SCCNij3 was derived from a primary human squamous cell carcinoma of the larynx (moderately to well differentiated). Tumor lines E102 and E106 were derived from two different primary human glioblastomas.

Viable 1-mm^3 tumor pieces from resection specimens were transplanted subcutaneously in nude mice (BALB/c ABom *nu* mouse). Tumors were passaged when they reached a diameter of 1 cm. For the oxygen measurements, tumors were transplanted in the right hind leg.

Calculation of tumor volume was based on the formula $(A \times B \times C \times \pi)/6$, where A, B and C are tumor diameters measured with calipers in three perpendicular directions.

Animals were kept in a specific-pathogen-free unit in accordance with institutional guidelines, and all animal experiments were conducted in accordance with the appropriate institutional and national guidelines.

Tumor specimens were stored in liquid nitrogen immediately after the pO_2 measurements until they were cut into 5-μm frozen sections. The sections were then stored at $-80°C$ until they were stained. Tumor tissue sections at the largest circumference of the tumor were analyzed.

Experimental Setup

During the measurements, the animals were kept under anesthesia to minimize any artifacts of pO_2 measurements due to movements of the

animals. An acrylic distributor for the anesthetic gas enflurane (Ethrane™) in admixture with a continuous flow of air was used. The setup was kept at a constant temperature of 33°C with a warm water mattress. The body temperature of the mice was recorded continuously during the experiments by a rectal probe (see below).

Tumor pO_2 Measurements

The recently developed and marketed fiber-optic oxygen-sensing device, OxyLite™ (Oxford Optronix™, Oxford, UK), was used to measure tumor pO_2. Details of the methodology of the fiber-optic oxygen tension measurements are given elsewhere[2] (*19, 20*). The pO_2 measurements are based on the principle that, after optical excitation of a luminophore, the half-life for a return to the ground state is inversely related to the oxygen tension. The luminophore used for this purpose is a ruthenium chloride complex. Blue light-emitting diodes are used as the source of excitation light, at around 450 nm. A single optical fiber guides the blue light as well as the resultant luminescence. The luminophore at the tip of the probe absorbs a proportion of the blue light. When the ruthenium chloride complex returns to the ground state, the emitted photons have a wavelength of around 590–620 nm. The response of the sensor to pO_2 is nonlinear and the probes therefore must be precalibrated. The probes that were used in the present experiments were precalibrated by the manufacturers.

The lifetime of the luminescence is also dependent on temperature. Therefore, all measurements are corrected automatically for differences in temperature using a thermocouple. In these experiments, mainly small tumors of 6–8 mm were used, and the temperature probe would thus have been located just underneath the skin. The temperature correction of the pO_2 measurements was therefore based on the rectal temperature (using a separate thermocouple) since it was felt that this was a better reference than the skin temperature. It was found that temperatures measured in the central part of the tumor were within 0.5°C of the rectal temperatures, even if measured over several hours (data not shown). The resulting error in the pO_2 measurements was less than 1 mmHg under these conditions.[2]

The fiber-optic probes were inserted in the tumor through a small 0.6-mm needle (23 gauge) and placed in the center of the tumor. After insertion, the needle was pulled back. In each tumor pO_2 measurements were performed in a single position; pO_2 values were determined from the plateau that was reached within 1 to 10 min after insertion of the fiber-optic pO_2 probe. The time needed to reach a plateau for the pO_2 value was not different among the three tumor lines. After the pO_2 measurements had reached a plateau for over 5 min, the pO_2 values were calculated as the average pO_2 over the next 5 min. The oxygen tension was measured in a total of 35 SCCNij3 tumors, 28 E102 gliomas, and 38 E106 gliomas.

Marker of Hypoxia

Pimonidazole hydrochloride [1-((2-hydroxy-3-piperidinyl)propyl)-2-nitroimidazole hydrochloride] was used at a dose of 80 mg/kg as a marker of hypoxia and was injected intravenously 20 min prior to the start of the pO_2 measurements (*33, 34*). Pimonidazole is a bioreductive chemical probe with an immuno-recognizable side chain. The addition of the first electron in bioreductive activation is reversibly inhibited by oxygen with a half-maximal pO_2 of inhibition of about 3 mmHg, with complete inhibition occurring at approximately 10 mmHg (*33*). Pimonidazole was injected in 13 of the 35 SCCNij3 tumor-bearing mice, 12 of the 28 E102 tumor-bearing mice, and 7 of the 38 E106 tumor-bearing mice.

Immunohistochemical Staining

After the sections were thawed, they were fixed in acetone for 10 min. Slides were then rinsed in phosphate-buffered saline (PBS). The sections were rinsed three times for 2 min each in PBS between all the consecutive steps of the staining procedure.

Endothelial Structures and Hypoxia Marker Pimonidazole

Sections were incubated overnight (16 h) at 4°C with undiluted 9F1 rat monoclonal antibody to mouse endothelium (*35*) together with rabbit anti-pimonidazole antiserum (*36, 37*) 1:200 in undiluted 9F1. Sections were then incubated for 60 min at room temperature with tetramethyl rhodamine isothiocyanate (TRITC)-conjugated goat anti-rat antiserum (Jackson Immuno Research Laboratories, West Grove, PA) 1:100 together with biotin-conjugated donkey anti-rabbit serum (Jackson Immuno Research Laboratories) 1:100 in PBS-B (PBS with 0.5% bovine serum albumin). This was followed by a 60-min pooled incubation at room temperature with TRITC-conjugated donkey anti-goat antiserum (Jackson Immuno Research Laboratories) and streptavidin-Alexa488 (Molecular Probes Inc. Eugene, OR), both 1:100 in PBS-B.

Scanning of Sections, Image Processing and Analysis of Parameters of Hypoxia

The tumor sections were scanned for quantitative analysis by a computerized digital image processing system as described elsewhere (*30, 32*). A high-resolution intensified solid-state camera on a fluorescence microscope (Zeiss Axioskop) with a computer-controlled motorized stepping stage was used. Tumor cross sections were scanned sequentially at a magnification of 100×, using different filters for the TRITC and Alexa488 signals. After each scan, which consisted of 36 or 64 fields (6 × 6 or 8 × 8, depending on the size of the tissue section) of 1.2 mm^2 each, one composite binary image was reconstructed from the individual microscope fields. The whole scanning procedure thus yielded two composite images from each tumor cross section: one showing hypoxic areas (pimonidazole) and one showing vascular structures (9F1). Finally a hematoxylin and eosin (H&E) staining of the tissue sections made it possible to draw a contour line around the tumor area while excluding nontumor tissue and areas of necrosis.

Determination of the hypoxic cell fraction was based on pimonidazole adduct binding. The hypoxic fraction was defined as the tissue area that stained positive for the hypoxic cell marker (pimonidazole) relative to the total tissue area (*32*).

Statistics

Linear least-squares regression analysis was used for calculation of the correlation between hypoxic fraction and mean pO_2. ANOVA was used for calculation of the differences in hypoxic fraction and pO_2 between the tumor lines. The statistical analyses were done on a Macintosh computer using the Statistica 4.0 software package.

RESULTS

Figure 1 shows an H&E-stained tumor section of tumor line SCCNij3 with a fiber optic oxygen probe overlaid. This figure gives an indication of the dimensions of the probe relative to the tissue architecture. The pO_2 measured is an average of the oxygen tension in the ruthenium chloride at the tip of the fiber-optic probe. The measuring volume consists of the tissue area directly adjacent to the tip of the probe. With an average cell size of 15 μm, a total amount of 400 cells would be lying adjacent to the tip of the fiber-optic probe (*38*).

Oxygen Tension and Tumor Size

Figure 2A is a plot of the cumulative pO_2 values obtained from all individual tumors of the three different tumor lines. With a median pO_2 of 2 mmHg, the squamous cell carci-

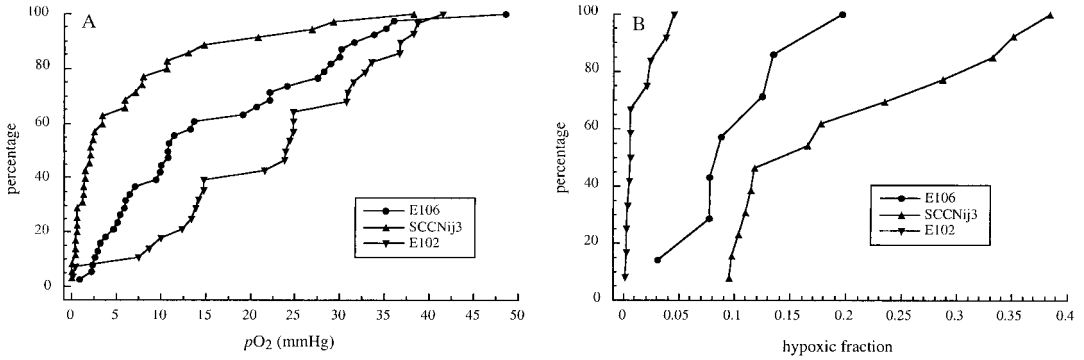

FIG. 2. Cumulative frequency (percentage) of pO_2 measurements by OxyLite™ (panel A) and hypoxic fraction determined by pimonidazole staining (panel B) of individual tumors of the human squamous cell carcinoma tumor line SCCNij3 and of the human glioblastoma tumor lines E102 and E106.

noma tumor line was the most hypoxic of the three tumor lines that were analyzed. The median pO_2 values of the two glioma tumor lines were 11 and 24 mmHg. The mean and median as well as the proportion of pO_2 values below 2.5, 5 and 10 mmHg are shown in Table 1. The differences in pO_2 values between the three tumor lines were statistically significant (ANOVA, $P = 0.002$). Most of the tumors used for these experiments had a diameter between 5.5 and 7 mm (the approximate volumes ranged from 80 to 200 mm^3). Within this relatively narrow range of tumor sizes, no correlation was found between tumor volume and the pO_2 measurements from the center of the tumors in any of the three tumor lines (Fig. 3).

Hypoxic Fraction

Figure 4 shows binary images of representative examples of the three tumor lines demonstrating the distribution of the stained pimonidazole adducts in the tumor section. Although tumor hypoxia staining was found throughout the tissue section in the SCCNij3 tumor, it was present predominantly in the center of the tumor. The arrows in Fig. 4 (SCCNij3) indicate a necrotic area in the center of the tumor. In the binary images, necrosis can be recognized as a red/yellow color as the result of nonspecific staining; this was confirmed by H&E staining of the same tissue section. The necrotic areas were excluded from the calculation of the hypoxic fraction.

A cumulative plot of the hypoxic fraction obtained from the individual tumors is shown in Fig. 2B. The median hypoxic fraction of SCCNij3 tumors was 0.14 (mean 0.20, range 0.1–0.38, $n = 13$). Glioma tumor line E102 showed little pimonidazole binding and had a median hypoxic fraction of 0.004 (mean 0.01, range 0.001–0.05, $n = 12$). Glioma tumor line E106 showed a diffuse patchy pattern of pimonidazole binding with no predominance in central or peripheral parts of the tumor. The median hypoxic fraction was 0.08 (mean 0.1, range 0.08–0.2, $n = 7$). In contrast to the SCCNij3 tumor, this tumor line showed hardly any necrosis. If necrosis was seen in E106 tumors at all (by means of H&E staining), it was not specifically located in the center of the tumor but rather in small areas throughout the tumor section. The differences in hypoxic fraction between the three tumor lines were statistically significant (ANOVA, $P < 0.05$).

Oxygen Tension and Hypoxic Fraction

The median hypoxic fraction relative to the median pO_2 for the three tumor lines is shown in Fig. 5. A strong correlation was found between the median pO_2 and the median hypoxic fraction as well as between the mean pO_2 and the mean hypoxic fraction of the three tumor lines (linear least-squares regression analysis, $P = 0.02$ for median pO_2 compared to median hypoxic fraction).

DISCUSSION

In this study, pO_2 measurements with a recently developed optical sensor (OxyLite™) were compared with bioreductive hypoxia marker binding (pimonidazole). The three different human tumor lines that were studied included one human head and neck squamous cell carcinoma and two human glioblastoma tumor lines grown as xenografts

TABLE 1
Oxygen Tension Characteristics of the Three Human Tumor Lines

	pO_2 (mmHg)					Percentage of pO_2 values		
Tumor line	Mean	Median	Range	n^a	SEM	≤2.5	≤5	≤10
SCCNij3	6.4	2	0–38	35	3.2	57	63	77
E106	16	11	0.8–42	38	4.2	8	21	45
E102	22	24	0–42	28	2.9	7	7	14

[a] Number of animals.

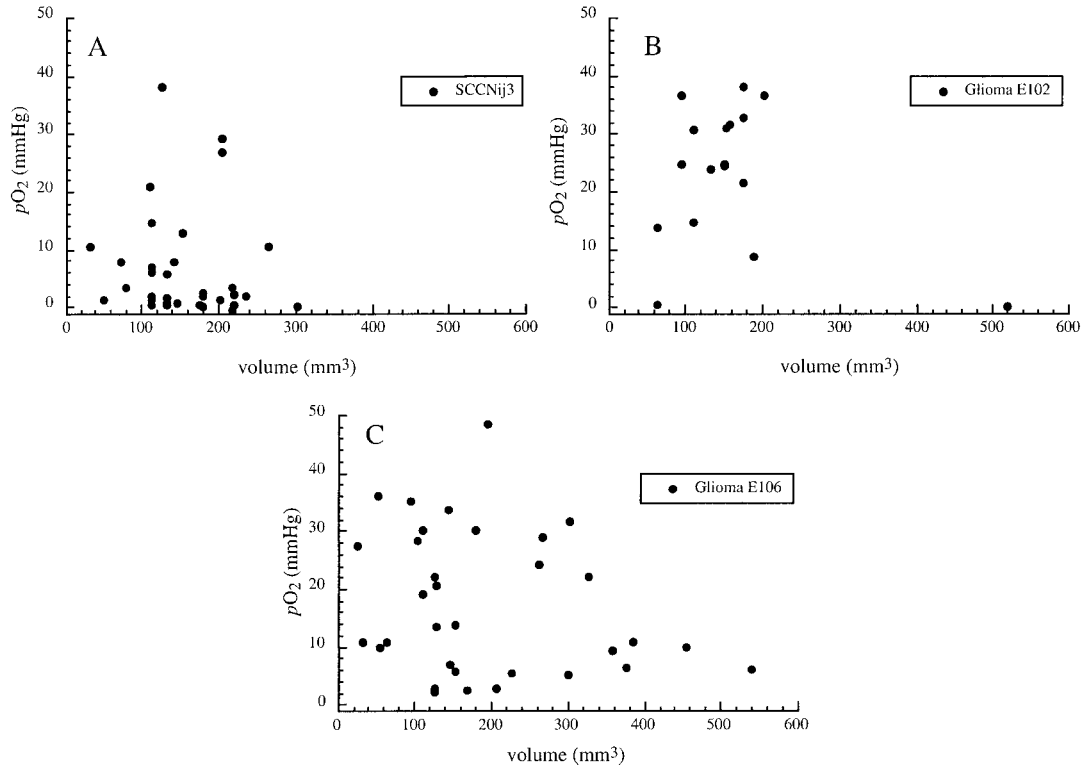

FIG. 3. Tumor pO_2 as a function of tumor volume. All data points represent pO_2 values measured at one position in the center of individual tumors of the human squamous cell carcinoma tumor line SCCNij3 (panel A) and of the human glioblastoma tumor lines E102 (panel B) and E106 (panel C).

in nude mice. Tumor hypoxia (pimonidazole staining) and pO_2 varied significantly between these three tumor lines. The measurements showed a good correlation between tumor pO_2 and binding of the bioreductive hypoxia marker pimonidazole.

The instrument most commonly used for direct pO_2 measurements in tissues is a polarographic oxygen microelectrode (Eppendorf™). These pO_2 measurements are based on the linear relationship between electrode currents and oxygen availability. This method has the advantage of a short acquisition time (fraction of a second). With the Eppendorf™ design, the polarographic microelectrode advances through the tissue with a varying step size, usually of the order of 0.4 to 0.7 mm, and acquires a reading at each step (*16, 18*). In this way, a large number of pO_2 measurements per tumor can be obtained within 10 to 15 min. A disadvantage of the microelectrodes is that they cannot remain at one position for continuous measurements because they consume oxygen; thus they may measure artificially low oxygen tensions after some time. Another disadvantage is that the accuracy decreases at lower oxygen tensions due to the weak electrical currents associated with the low oxygen concentrations (*20*). The OxyLite™ system has overcome some of these limitations. There is no oxygen consumption, which allows the probe to stay in the same position for a prolonged time (hours). The relationship between the lifetime of the luminescence and the oxygen tension is nonlinear. At low pO_2 levels, where the degree of quenching is least, the lifetime and signal amplitudes are greatest, which results in an enhanced accuracy at low pO_2 levels. A disadvantage of this nonlinear relationship is that the probes need to be precalibrated and the measurements become less precise at higher pO_2 levels (*19*).

At the moment, the OxyLite system is not suited for sampling multiple sites in one tumor. Another disadvantage of this methodology is that it can take 1 to 10 min after insertion of the optic fiber before the pO_2 value reaches a plateau. This period is probably necessary for the tissue to be restored after the mechanical damage caused by inserting the pO_2 probe. It is unclear whether this is a disadvantage only for the fiber-optic probes with a rounded tip, or if this is a process that also occurs with needle-type sensors with sharp tips, such as the Eppendorf™. However, for the Oxylite system, once the pO_2 value has reached a plateau, the time to respond to a change in pO_2, caused for instance by carbogen breathing, is less than 1 min.[2] This favors the hypothesis that this phenomenon of reaching a plateau is likely to be caused by a mechanical disruption or compression, which also occurs with other types of invasive pO_2 measurements (*39*). As soon as a stepping device for moving the fiber-optic probe through tissues becomes available, a direct comparison of the two methodologies will be possible.

The bioreductive compound pimonidazole was used as marker of hypoxia. Initially pimonidazole was used in the clinic as a hypoxic cell sensitizer. However, its effectiveness

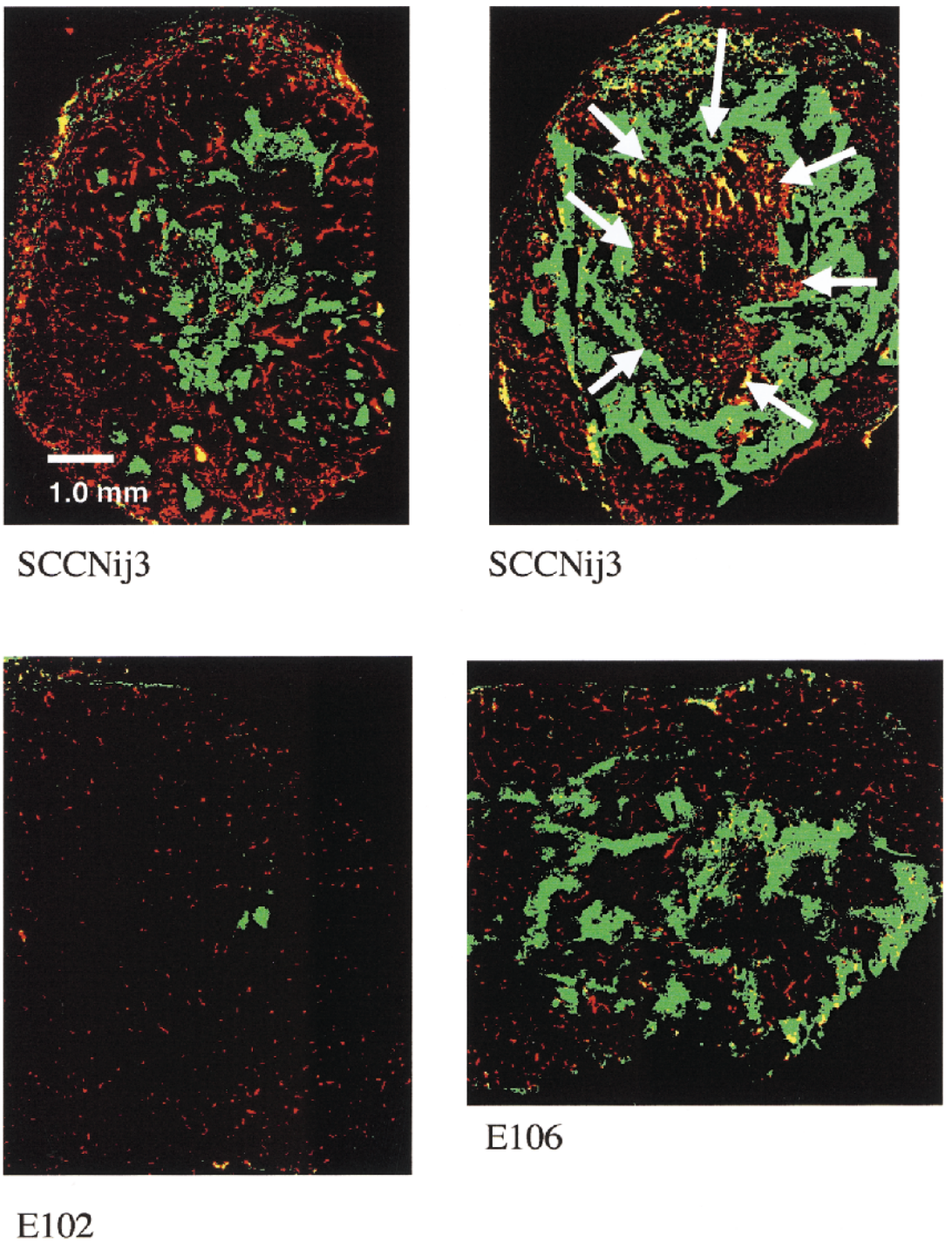

FIG. 4. Pseudo-colored composite images reconstructed after scanning for the vascular structures (9F1, red) and hypoxia (pimonidazole, green) of complete sections of the human squamous cell carcinoma xenograft tumor line SCCNij3 and the human glioblastoma tumor lines E102 and E106. Determination of the characteristics of the vasculature is based on analysis of images at 100× magnification. The size of the vessels in the glioblastoma lines is smaller than in line SCCNij3. The differences in vascular surface observed are due to the resolution of the images. Necrotic areas were identified on the same tissue sections by means of H&E staining and are indicated by arrows. The scale bar refers to all four images.

was not proven in clinical trials (*40*). After development of an antibody against pimonidazole (*36*), it has been tested extensively in tumor models as a hypoxic cell marker, and it was recently reintroduced into the clinic for this reason. The characteristics of pimonidazole are very similar to misonidazole (*33*), with a steep increase in the amount of reduction below a pO_2 of 10 mmHg (*41*).

With pimonidazole as hypoxia marker, the distribution pattern of hypoxic regions throughout a tissue section can be studied (*32*). Although data on the diffusion distance of

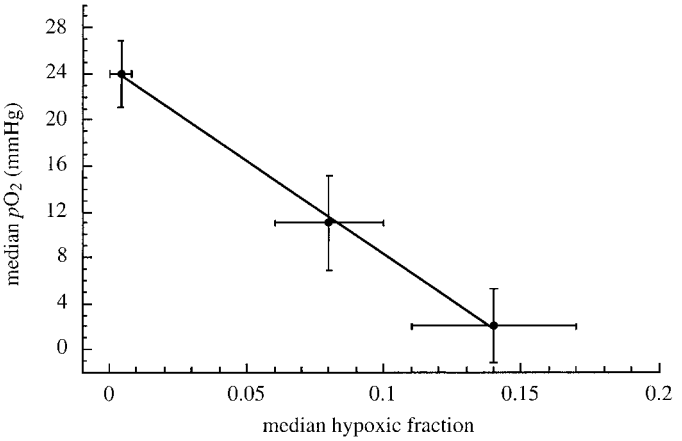

FIG. 5. Median tumor pO_2 as a function of median hypoxic fraction of the human squamous cell carcinoma tumor line SCCNij3 and of the human glioblastoma tumor lines E102 and E106 (±SEM).

bioreductive hypoxic cell markers are sparse, it was shown in a study with the 2-nitroimidazole AF-2 that these markers can diffuse up to 400 μm through excised tumors cubes of 1–2 mm (*15*). Pimonidazole staining was more centrally located in the squamous cell carcinoma line SCCNij3 compared with glioma line E106 (Fig. 4). Since the pO_2 was measured in the central part of the tumor, the probability of measuring in a hypoxic area is higher in SCCNij3 tumors than in E106 tumors (compare Fig. 3A and C).

Extensive necrosis in the center of the tumor was found in 5 of the 20 SCCNij3 tumors with pO_2 readings below 2.5 mmHg. The majority of necrotic areas were located in the center of this tumor, and these necrotic areas were also larger in SCCNij3 tumors compared to E106 tumors; thus there is a probability that irrelevant measurements are being made in necrotic areas of the SCCNij3 tumors. In fact, this may have been the case in 5 of 20 tumors that showed readings below 2.5 mmHg. The necrotic areas are excluded from the analysis of the hypoxic fraction, because in necrotic areas pimonidazole is not reduced. Especially in tumor line SCCNij3 the necrotic as well as the hypoxic areas were located predominantly in the center of the tumor. This may be one reason why 80% of the pO_2 values in this tumor were below 10 mmHg, with a median pimonidazole binding-based hypoxic fraction of 0.14. Another reason for this discrepancy may be that pO_2 measurements with OxyLite originate from the space around the tip of the probe, whereas pimonidazole is analyzed in a two-dimensional way at the cellular level. This could also explain the discrepancy between Eppendorf-based pO_2 measurements and the hypoxic fraction determined with pimonidazole (*33*). It is likely that hypoxia at the cellular level is correlated with global tumor pO_2. A higher impact of a decrease in (cellular) oxygen consumption relative to increased blood perfusion with a higher oxygen tension on the tumor pO_2 was suggested by a theoretical simulation (*42*).

Raleigh *et al.* (*33*) recently published the results of a study in which pimonidazole binding was compared with Eppendorf™-based pO_2 measurements. Different levels of oxygenation were induced in the C3H mouse mammary carcinoma. Either the animals were treated with hydralazine or were allowed to breathe different gas mixtures such as air, carbogen and pure oxygen, or hypoxia was induced by clamping the blood supply to tumors. A good correlation was found between radiobiological hypoxia, analyzed with the paired survival curve method, pimonidazole binding, and pO_2 measurements (Eppendorf™) (*33*). The correlation between pimonidazole adduct binding and Eppendorf™-based pO_2 was strongest if the pimonidazole hypoxic fraction was compared with the percentage of pO_2 readings below 10 mmHg. The correlation between the hypoxic fraction and the mean pO_2 of each tumor was weaker.

For the experiments reported here, the hypoxic tumor fractions were calculated in the same tumors after measurement of pO_2. There was a good correlation between median pO_2 and median hypoxic fraction (Fig. 5). However, extensive heterogeneity of well and poorly oxygenated regions within each tumor line were found with the pimonidazole binding method which is illustrated in Fig. 4. Although we did find a good correlation between the results of the two methodologies, they are clearly different in nature, each having specific strengths and weaknesses. The strength of the hypoxia marker binding method obviously is the high spatial resolution. The advantage of the OxyLite™ system is that absolute pO_2 values can be obtained and, perhaps most important, that continuous measurements can be taken from the same position over prolonged periods. This will give dynamic information on the oxygenation status of tumors with the possibility for better monitoring of the effects of oxygenation-modifying treatments. Spatial information can be increased by using multiple probes per tumor or by adding a stepping stage on the OxyLite™ device as with the Eppendorf™ system.

In a number of studies, parameters derived from Eppendorf™-based pO_2 measurements have been identified that can predict treatment outcome (*17, 18, 27*). Although statistically significant differences in pretreatment characteristics have been found, it still is not possible to use these

parameters for pretreatment selection on an individual basis. An assay to test the effect of treatments modifying the oxygenation status of a tumor, such as administration of drugs to increase tumor blood perfusion, or carbogen breathing, in an individual patient has the potential of being predictive for treatment outcome. For oxygen tension measurements, the newly developed time-resolved fiber-optic pO_2 measuring OxyLite™ allows the study of pO_2 but with the constraint that only a limited number of measurements per tumor are possible. In the present study, a good correlation between time-resolved fiber-optic pO_2 measurements and tumor hypoxic fraction based on bioreductive chemical probe binding was found for three human tumors that varied significantly in their oxygenation status. Although a significant difference in pO_2 and hypoxic fraction between the three lines was found, the results also showed a large variation within each tumor line. This indicates that multiple measurements per tumor or per tumor line are necessary for global assessment of tumor hypoxia.

CONCLUSION

The tumor microenvironment is a dynamic system, and it is important to quantify dynamic changes in the tumor microenvironment to better understand the biology of tumors. The major strength of the OxyLite™ lies in the ability to monitor pO_2 in the same tumor area for a prolonged period; this aspect is being investigated further in ongoing experiments. A combination of a bioreductive hypoxic cell marker, for global assessment of tumor hypoxia, in combination with continuous pO_2 measurements with the OxyLite™ may be helpful in selecting patients on an individual basis for oxygenation-modifying treatments.

ACKNOWLEDGMENTS

9F1 (rat monoclonal antibody to mouse endothelium) was a gift from Dr. G. van Muijen of the Department of Pathology, University Hospital Nijmegen, Nijmegen, the Netherlands. We thank Dr. J. A. Raleigh (Department of Radiation Oncology, University of North Carolina School of Medicine, Chapel Hill, NC) for supplying pimonidazole. We thank Oxford Optronics Ltd. for supplying the fiber-optic oxygen probes. We thank the Central Animal Laboratory for excellent animal care. We thank P. F. J. W. Rijken for image analysis support. This investigation was supported by the Dutch Cancer Society and by the European Community, BIOMED II concerted action (BMH4–98–3006).

Received: March 23, 2000; accepted: June 27, 2000

REFERENCES

1. J. C. Mottram, A factor of importance in the radiosensitivity of tumours. *Br. J. Radiol.* **60**, 606–614 (1936).
2. L. H. Gray, A. D. Conger, M. Ebert, S. Hornsey and O. C. A. Scott, The concentration of oxygen dissolved in tissues at the time of irradiation as a factor in radiotherapy. *Br. J. Radiol.* **26**, 638–648 (1953).
3. J. M. Henk, Late results of a trial of hyperbaric oxygen and radiotherapy in head and neck cancer: a rationale for hypoxic cell sensitizers? *Int. J. Radiat. Oncol. Biol. Phys.* **12**, 1339–1341 (1986).
4. E. R. Watson, K. E. Halnan, S. Dische, M. I. Saunders, I. S. Cade, J. B. McEwen, G. Wiernik, D. J. Perrins and I. Sutherland, Hyperbaric oxygen and radiotherapy: A medical research council trial in carcinoma of the cervix. *Br. J. Radiol.* **51**, 879–887 (1978).
5. J. Overgaard, H. Sand-Hansen, M. Overgaard, L. Bastholt, A. Berthelsen, L. Specht, B. Lindeløv and K. Jørgensen, A randomized double-blind phase III study of nimorazole as a hypoxic radiosensitizer of primary radiotherapy in supraglottic larynx and pharynx carcinoma. Results of the Danish Head and Neck Cancer Study (DAHANCA) protocol 5-85. *Radiother. Oncol.* **46**, 135–146 (1998).
6. J. H. A. M. Kaanders, L. A. M. Pop, H. A. M. Marres, J. Liefers, F. J. A. Van den Hoogen, W. A. J. Van Daal and A. J. van der Kogel, Accelerated radiotherapy with carbogen and nicotinamide (ARCON) for laryngeal cancer. *Radiother. Oncol.* **48**, 115–122 (1998).
7. J. Bussink, J. H. A. M. Kaanders and A. J. van der Kogel, Clinical results and tumor microenvironmental effects of accelerated radiotherapy with carbogen and nicotinamide. *Acta Oncol.* **38**, 875–882 (1999).
8. M. Höckel, K. Schlenger, B. Aral, M. Mitze, U. Schäffer and P. Vaupel, Association between tumor hypoxia and malignant progression in advanced carcinoma of the uterine cervix. *Cancer Res.* **56**, 4509–4515 (1996).
9. D. M. Brizel, G. S. Scully, J. M. Harrelson, L. J. Layfield, J. M. Mean, L. R. Prosnitz and M. W. Dewhirst, Tumor oxygenation predicts for the likelihood of distant metastases in human soft tissue sarcoma. *Cancer Res.* **56**, 941–943 (1996).
10. K. Sundfor, H. Lyng and E. K. Rofstad, Tumor hypoxia and vascular density as predictors of metastasis in squamous cell carcinoma of the uterine cervix. *Br. J. Cancer* **78**, 822–827 (1998).
11. R. M. Sutherland, Tumor hypoxia and gene expression: Implications for malignant progression and therapy. *Acta Oncol.* **37**, 567–574 (1998).
12. T. Y. Reynolds, S. Rockwell and P. M. Glazer, Genetic instability induced by the tumor microenvironment. *Cancer Res.* **56**, 1754–1757 (1996).
13. L. M. Van Putten and R. F. Kallman, Oxygenation status of a transplantable tumor during fractionated radiation therapy. *J. Natl. Cancer Inst.* **40**, 441–451 (1968).
14. J. E. Moulder and S. Rockwell, Hypoxic fractions of solid tumors: Experimental techniques, methods of analysis and a survey of existing data. *Int. J. Radiat. Oncol. Biol. Phys.* **10**, 695–712 (1984).
15. P. L. Olive, Radiation-induced reoxygenation in the SCC VII murine tumour: Evidence for a decrease in oxygen consumption and an increase in tumor perfusion. *Radiother. Oncol.* **32**, 37–46 (1994).
16. P. Vaupel, K. Schlenger, C. Knoop and M. Höckel, Oxygenation of human tumors: evaluation of tissue oxygen distribution in breast cancers by computerized O_2 tension measurements. *Cancer Res.* **51**, 3316–3322 (1991).
17. M. Höckel, C. Knoop, K. Schlenger, B. Vorndran, E. Baussmann, M. Mitze, P. G. Knapstein and P. Vaupel, Intratumoral pO_2 predicts survival in advanced cancer of the uterine cervix. *Radiother. Oncol.* **26**, 45–50 (1993).
18. M. Nordsmark, M. Overgaard and J. Overgaard, Pretreatment oxygenation predicts radiation response in advanced squamous cell carcinoma of the head and neck. *Radiother. Oncol.* **41**, 31–39 (1996).
19. W. K. Young, B. Vojnovic and P. Wardman, Measurement of oxygen tension in tumours by time-resolved fluorescence. *Br. J. Cancer* **74** (Suppl.), S256–S259 (1996).
20. D. R. Collingridge, W. K. Young, B. Vojnovic, P. Wardman, E. M. Lynch, S. A. Hill and D. J. Chaplin, Measurement of tumor oxygenation: A comparison between polarographic needle electrodes and a time-resolved luminescence-based optical sensor. *Radiat. Res.* **147**, 329–334 (1997).
21. A. Long, J. Parrick and R. J. Hodgkiss, An efficient procedure for the 1-alkylation of 2-nitroimidazoles and the synthesis of a probe for hypoxia in solid tumors. *Synthesis* **9**, 709–713 (1991).
22. J. A. Raleigh, G. G. Miller, A. J. Franko, C. J. Koch, A. F. Fuciarelli and D. A. Kelly, Fluorescence immunohistochemical detection of

hypoxic cells in spheroids and tumours. *Br. J. Cancer* **56**, 395–400 (1987).

23. C. J. Koch, S. M. Evans and E. M. Lord, Oxygen dependence of cellular uptake of EF5 [2-(2-nitro-^{1}H-imidazol-1-yl)-*N*-(2,2,3,3,3-pentafluoropropyl)acetamide]: Analysis of drug adducts by fluorescent antibodies vs bound radioactivity. *Br. J. Cancer* **72**, 869–874 (1995).

24. F. Goda, J. A. O'Hara, E. S. Rhodes, K. J. Liu, J. F. Dunn, G. Bacic and H. M. Swartz, Changes of oxygen tension in experimental tumors after a single dose of X-ray irradiation. *Cancer Res.* **55**, 2249–2252 (1995).

25. B. M. Fenton, Effects of carbogen plus fractionated irradiation on KHT tumor oxygenation. *Radiother. Oncol.* **44**, 183–190 (1997).

26. R. A. Gatenby, H. B. Kessler, J. S. Rosenblum, L. R. Coia, P. J. Molodofsky, W. H. Hartz and G. J. Broder, Oxygen distribution in squamous cell carcinoma metastases and its relationship to outcome of radiation therapy. *Int. J. Radiat. Oncol. Biol. Phys.* **14**, 831–838 (1988).

27. D. M. Brizel, G. S. Sibley, L. R. Prosnitz, R. L. Scher and M. W. Dewhirst, Tumor hypoxia adversely affects the prognosis of carcinoma of the head and neck. *Int. J. Radiat. Oncol. Biol. Phys.* **38**, 285–289 (1997).

28. H. B. Stone, J. M. Brown, T. L. Phillips and R. M. Sutherland, Oxygen in human tumors: Correlations between methods of measurement and response to therapy. Summary of a workshop held November 19–20, 1992, at the National Cancer Institute, Bethesda, Maryland. *Radiat. Res* **136**, 422–434 (1993). [meeting report]

29. W. J. Whalen, J. Riley and P. A. Nair, A microelectrode for measuring intracellular pO_2. *J. Appl. Physiol.* **23**, 798–801 (1967).

30. P. F. J. W. Rijken, H. J. J. A. Bernsen and A. J. van der Kogel, Application of an image analysis system to the quantitation of tumor perfusion and vascularity in human glioma xenografts. *Microvasc. Res.* **50**, 141–153 (1995).

31. J. Bussink, J. H. A. M. Kaanders, P. F. J. W. Rijken, C. A. Martindale and A. J. van der Kogel, Multi-parameter analysis of vasculature, perfusion and proliferation in human tumour xenografts. *Br. J. Cancer* **77**, 57–64 (1998).

32. J. Bussink, J. H. A. M. Kaanders, P. F. J. W. Rijken, R. J. Hodgkiss and A. J. van der Kogel, Vascular architecture and microenvironmental parameters in human squamous cell carcinoma xenografts: effects of carbogen and nicotinamide. *Radiother. Oncol.* **50**, 173–183 (1999).

33. J. A. Raleigh, S-C. Chou, G. E. Arteel and M. R. Horsman, Comparisons among pimonidazole binding, oxygen electrode measurements and radiation response in C3H mouse tumors. *Radiat. Res.* **151**, 580–589 (1999).

34. R. E. Durand and J. A. Raleigh, Identification of non-proliferating but viable hypoxic tumor cells in vivo. *Cancer Res.* **58**, 3547–3550 (1998).

35. J. R. Westphal, R. G. M. Van't Hullenaar, J. A. W. M. Van der Laak, I. M. H. A. Cornelissen, L. J. M. Schalkwijk, G. N. P. Van Muijen, P. Wesseling, P. C. M. De Wilde, D. J. Ruiter and R. M. W. De Waal, Vascular density in melanoma xenografts correlates with vascular permeability factor expression but not with metastatic potential. *Br. J. Cancer* **76**, 561–570 (1997).

36. G. E. Arteel, R. G. Thurman, J. M. Yates and J. A. Raleigh, Evidence that hypoxia markers detect oxygen gradients in liver: Pimonidazole and retrograde perfusion in rat livers. *Br. J. Cancer* **72**, 889–895 (1995).

37. C. Azuma, J. A. Raleigh and D. E. Thrall, Longevity of pimonidazole adducts in spontaneous canine tumors as an estimate of hypoxic cell lifetime. *Radiat. Res.* **148**, 35–42 (1997).

38. J. R. Griffiths and S. P. Robinson, The OxyLite: A fibre-optic oxygen sensor. *Br. J. Radiol.* **72**, 627–630 (1999).

39. J. A. Raleigh, M. W. Dewhirst and D. E. Thrall, Measuring tumor hypoxia. *Semin. Radiat. Oncol.* **6**, 37–45 (1996).

40. S. Dische, D. Machin and D. Chassagne, on behalf of the Medical Research Council Working Party on advanced carcinoma of the cervix, A trial of Ro 03–8799 (pimonidazole) in carcinoma of the uterine cervix: an interim report of the Medical Research Council Working Party on advanced carcinoma of the cervix. *Radiother. Oncol.* **26**, 93–103 (1993).

41. M. W. Gross, U. Karbach, K. Groebe, A. J. Franko and W. Mueller-Klieser, Calibration of misonidazole labeling by simultaneous measurement of oxygen tension and labeling density in multicellular spheroids. *Int. J. Cancer* **61**, 567–573 (1995).

42. T. S. Secomb, R. Hsu, E. T. Ong, J. F. Gross and M. W. Dewhirst, Analysis of the effect of oxygen supply and demand on hypoxic fraction in tumors. *Acta Oncol.* **34**, 313–316 (1995).